RESEARCH PAPER

Channels 8:5, 433–443; September/October 2014; © 2014 Taylor & Francis Group, LLC

Functional formation of heterotypic gap junction channels by connexins-40 and -43

Xianming Lin[†], Qin Xu[††], and Richard D Veenstra*

Department of Pharmacology; SUNY Upstate Medical University; Syracuse, NY USA

[†]Current address: Leon H Charney Division of Cardiology; New York University School of Medicine; New York, NY USA

[††]Current address: Department of Psychiatry, Faculty of Medicine; The University of British Columbia; Vancouver, BC Canada

Keywords: Connexin40, connexin43, gap junctions, heterotypic, spermine, transjunctional voltage gating

Abbreviations: Cx40, connexin40; Cx43, connexin43; N2a, mouse Neuro2a; V_j, transjunctional voltage; G_j, normalized junctional conductance; wt, wild-type; NT, N-terminal domain; mCx30.2/hCx31.9, mouse connexin30.2/human connexin31.9; Cx45, connexin45; Cx37, connexin37; Rin, renal insulinoma; RT-PCR, real-time PCR; GAPDH, glyceraldehyde-3-phosphate dehydrogenase; $G_{j,max}$, maximum normalized g_j; $G_{j,min}$, mimimum normalized g_j; $V_{1/2}$, half-inactivation voltage; I_j, junctional current; g_j, junctional conductance; τ_{decay}, exponential decay time constant; P_{open}, open probability; K_{on}, inactivation on-rate; γ_j, single gap junction channel conductance; pS, picoSiemen; EDTA, Ethylenediaminetetraacetic acid; i_j, single gap junction channel current; E1, first extracellular loop domain; FITC, fluorescein isothiocyante; TRITC, tetramethylrhodamine isothiocyanate; V_1 and V_2, command voltage clamp potentials for cell 1 and cell 2; I_1 and I_2, whole cell currents for cell 1 and cell 2; R_{el1} and R_{el2}, whole cell patch electrode resistance values for cell 1 and cell 2; ΔI_2, change in I_2 in response to an applied Vj gradient produced by changing V_1; TBS, Tris buffered saline.

Connexin40 (Cx40) and connexin43 (Cx43) are co-expressed in the cardiovascular system, yet their ability to form functional heterotypic Cx43/Cx40 gap junctions remains controversial. We paired Cx43 or Cx40 stably-transfected N2a cells to examine the formation and biophysical properties of heterotypic Cx43/Cx40 gap junction channels. Dual whole cell patch clamp recordings demonstrated that Cx43 and Cx40 form functional heterotypic gap junctions with asymmetric transjunctional voltage (V_j) dependent gating properties. The heterotypic Cx43/Cx40 gap junctions exhibited less V_j gating when the Cx40 cell was positive and pronounced gating when negative. Endogenous N2a cell connexin expression levels were 1,000-fold lower than exogenously expressed Cx40 and Cx43 levels, measured by real-time PCR and Western blotting methods, suggestive of heterotypic gap junction formation by exogenous Cx40 and Cx43. Imposing a [KCl] gradient across the heterotypic gap junction modestly diminished the asymmetry of the macroscopic normalized junctional conductance – voltage (G_j-V_j) curve when [KCl] was reduced by 50% on the Cx43 side and greatly exacerbated the V_j gating asymmetries when lowered on the Cx40 side. Pairing wild-type (wt) Cx43 with the Cx40 E9,13K mutant protein produced a nearly symmetrical heterotypic G_j-V_j curve. These studies conclusively demonstrate the ability of Cx40 and Cx43 to form rectifying heterotypic gap junctions, owing primarily to alternate amino-terminal (NT) domain acidic and basic amino acid differences that may play a significant role in the physiology and/or pathology of the cardiovascular tissues including cardiac conduction properties and myoendothelial intercellular communication.

Introduction

Gap junctions provide a direct pathway for passage of ions and small molecules between cells. Gap junction channels are formed by the docking of 2 connexons from adjacent cells, with each connexon, or connexin hemichannel, being formed by a hexamer of connexin subunits. There are 21 connexin genes in the mammalian genome and most cells express multiple connexins, resulting in a variety of gap junction channel configurations, including homotypic (same connexin isoform in both hemichannels), heterotypic (6 identical connexins in each hemichannel, but 2 different connexin hemichannels), or heteromeric (different connexins in at least one hemichannel) gap junction channels. Heterogeneous (heterotypic or heteromeric) gap junction channel formations have been demonstrated in mammalian tissues or in exogenous expression systems, although the functional capacity for connexins to heteromerically or heterotypically interact is only partially understood.[1-7] The functional consequences of heterologous gap junction formation on intercellular communication are partially understood. It has been reported that heterogeneous connexin channel formations sometimes display disparate biophysical and regulatory behaviors from the properties of the corresponding

*Correspondence to: Richard D Veenstra; Email: veenstrr@upstate.edu
Submitted: 01/20/2014; Revised: 07/10/2014; Accepted: 07/15/2014
http://dx.doi.org/10.4161/19336950.2014.949188

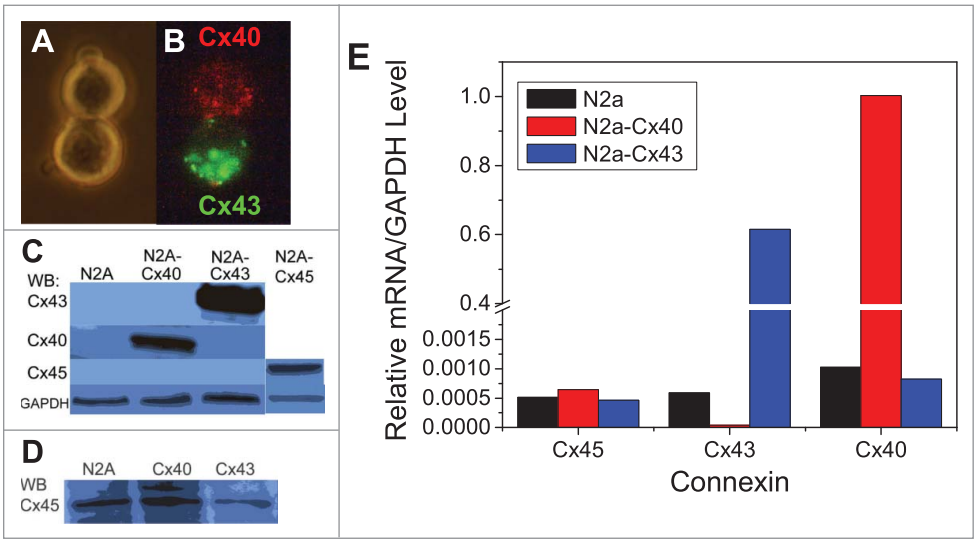

Figure 1. Bright-field (**A**) and epifluorescent (**B**) illumination of a heterotypic Cx40/Cx43 N2a cell pair after membrane labeling with and 24 hours in culture. (**C**) Western blots for Cx40, Cx43, and Cx45 protein expression in parental N2a (left lane), stable rat Cx40-N2a clone (left center lane), stable rat Cx43-N2a clone (right center lane), or transiently expressed murine Cx45 in parental N2a cells (right lane) relative to GAPDH. No endogenous Cx40, Cx43, or Cx45 expression was detected with picomole sensitive detection kit. (**D**) Endogenous Cx40, Cx43, and Cx45 was detectable with femtomolar detection. E, Real-time PCR results for endogenous murine Cx45 or exogenous rat Cx40 or Cx43 mRNA expression in parental or stable Cx N2a cell clones relative to GAPDH. Exogenously expressed Cx43 or Cx40 mRNA levels were 0.6–1.0 times the GAPDH level in their respective stable cell clones whereas endogenous Cx mRNA levels were <0.001 in all parental and stable N2a cell clones.

components, including voltage-dependent gating and chemical gating, single channel conductance, selectivity and permeability, and regulation.[8-11] These functional differences suggest that heterologous gap junction might participate in the physiology and/or pathology of tissues.[12,13]

In the cardiovascular system, 5 different connexins (mCx30.2/hCx31.9, Cx40, Cx43, Cx45, and Cx37) have been identified. Some of these connexins can form functional heteromeric or heterotypic gap junction channels. For example, Cx45 can form heterotypic channels with Cx43 or Cx40;[8-10] Cx30.2 can form heteromeric gap junction channels with the other cardiac connexins;[14] and Cx43 can form functional heteromeric channels with Cx45 or Cx37.[15,16] However, whether Cx40 and Cx43 can form functional heterogeneous channels is controversial even though they are co-expressed throughout the cardiovascular system. Several studies report that Cx40 and Cx43 are unable to form functional heterotypic channel in *Xenopus* oocytes and HeLa cells;[17,18] some other studies show that Cx40 and Cx43 can form heterotypic gap junction channels in HeLa or Rin (renal insulinoma) cells with asymmetrical voltage gating properties and intermediate selective permeabilities.[11,19-21] Rackauskas et al. reported that Cx40 and Cx43 do not make functional heterotypic gap junctions and suggested that endogenous Cx45 may mediate these supposed interactions.[10] In this study, we utilized Cx43 or Cx40 transfected mouse Neuro2a (N2a) cells, which express ≈1,000-fold lower levels of endogenous Cx45, to demonstrate that Cx43 and Cx40 can form functional heterotypic gap junction channels. The biophysical properties (such as voltage gating, inactivation kinetics, single channel conductance and spermine block) of this heterotypic formation are different from the behaviors of homotypic Cx43 or Cx40 gap junction channels. These differential properties may influence the physiology and/or pathology of the cardiovascular tissues (e.g. atrium, myoendothelium) and play a significant role in the myocardial conduction properties.

Results

Expression of endogenous connexins in N2a cells

To determine the endogenous levels of Cx40, Cx43 or Cx45 protein expression in N2a cells, immunoblotting procedures with picomole or femtomole-sensitive detection kits were performed. N2a-Cx40, N2a-Cx43, or murine Cx45-transiently transfected parental N2a cells were blotted as positive controls for detection of Cx40, Cx43 and Cx45. No endogenous Cx40, Cx43, or Cx45 expression was detected with picomole sensitive detection in untransfected N2a cells (**Fig. 1C**). Endogenous Cx45 protein expression was detectable only with femtomolar sensitivity (**Fig. 1D**).

Cx40, Cx43 and Cx45 mRNA expression levels were also examined by real-time PCR (RT-PCR) analysis in parental N2a cells and stable N2a-Cx40 or N2a-Cx43 cell clones. Exogenously expressed Cx43 or Cx40 mRNA levels were 0.6 -1.0 times the GAPDH level in their respective stable cell clones, whereas the endogenous Cx40, Cx43, and Cx45 mRNA levels were ≤0.001 relative to GAPDH mRNA levels in all parental and stable N2a cell clones (**Fig. 1E**). Endogenous Cx45 mRNA levels did not change with exogenous expression of Cx40 or Cx43.

Voltage-dependent gating

To determine the voltage-dependent gating properties of heterotypic Cx43/Cx40 gap junction channels, the steady-state G_j-V_j relationship was examined with a 200 msec/mV continuous V_j staircase of ±120 mV from 7 heterotypic Cx43/Cx40 cell pairs and the averaged G_j-V_j curve was fitted with a Boltzmann equation:

$$G_j = [G_{j,max} \cdot [\exp(zF/RT \cdot (V_j - V_{1/2}))] + G_{j,min}]/[1 + [\exp(zF/RT \cdot (V_j - V_{1/2}))]]$$

where $G_{j,max}$ is the normalized maximum G_j, $G_{j,min}$ is the residual voltage-insensitive portion of G_j achieved over the examined

V_j range, $V_{1/2}$ = the half-inactivation voltage, z is the valence in elementary charge units (q), F is Faraday's constant (in coulombs/mol), R is the molar gas constant [in J/(mol · K)], T was temperature (in K).

When N2a-Cx43 cells were paired with N2a-Cx40 cells, there was a significant asymmetry in voltage gating response (**Figs. 2A**, **B**). To pool the data from individual experiments, V_j was defined relative to the N2a-Cx40 cell. When the N2a-Cx40 cell voltage was relative negative (Cx43 V_j positive), the steady-state junctional current–voltage (I_j–V_j) relationships exhibited rectification, as indicated by a near zero $G_{j,min}$ and decreased $V_{1/2}$ values in the corresponding G_j–V_j curves. $G_{j,min} = 0.069 \pm 0.002$ and $V_{1/2} = -35.5 \pm 0.1$ (**Fig. 2B**, **Table 1**). These values are much lower than those of the homotypic Cx43 gap junction channels.[22] When the N2a-Cx40 cell voltage was relative positive (Cx43 V_j negative), there was an overall decrease in V_j gating with $G_{j,min} = 0.253 \pm 0.009$ and $V_{1/2} = +89.2 \pm 0.3$, higher than the values of homotypic Cx40 gap junctions (**Fig. 2B**, **Table 1**).[23] The average g_j was 1.20 ± 0.25 nS (mean ± s.d., n = 7).

We previously demonstrated that asymmetrical alterations in the transjunctional salt gradient for permeable ions results in an electrochemical diffusion potential across a gap junction and produces a noticeable asymmetry in the V_j-dependent gating properties of a homotypic gap junction.[24] Here we examined whether asymmetric alterations in the internal [KCl] pipette solutions could reduce or accentuate the shift in the heterotypic Cx43/Cx40 gap junction G_j–V_j curve. Again, V_j was defined relative to the N2a-Cx40 cell in these experiments, and [KCl] was unilaterally lowered from 140 mM to 70 mM. When 50% [KCl] was present on the Cx40-side, the asymmetric V_j-dependent gating of the heterotypic Cx43/Cx40 gap junction increased relative to symmetrical ionic conditions (**Figs. 2C**,**D** and **Table 1**). The average g_j was 0.51 ± 0.17 nS for these experiments (n = 6). When 50% [KCl] was present on the Cx43-side, the V_j-dependent gating asymmetry diminished slightly. The average g_j was 0.61 ± 0.13 nS (n = 6).

The best evidence thus far in favor of Cx43/Cx40 heterotypic gap junction formation in opposition to intermediary interactions with Cx45 is the ≥0.1% relative Cx45 mRNA or protein expression levels in N2a cells. To verify the formation of Cx43/Cx40 heterotypic gap junctions, we paired wild-type (wt) Cx43 with the previously described mutant Cx40E9,13K protein that mimicked the unilateral 2 mM spermine block of wt Cx40 gap junctions when paired with wt Cx40, presumably by reversing the polarity of Cx40 V_j-dependent gating.[25] The V_j gating properties were determined as before and the heterotypic Cx43/Cx40E9,13K gap junctions displayed relatively symmetrical V_j-gating properties when compared to their heterotypic wt Cx40/Cx43 counterparts, under symmetrical or asymmetrical [KCl] conditions (**Fig. 2F**, **Table 1**). The average g_j was 3.90 ± 1.84 nS for these experiments (mean ± s.d., n = 3).

Inactivation kinetics

The first order inactivation kinetics of these heterotypic Cx43/Cx40 gap junctions were measured using V_j pulses between −40 and −140 mV applied to either the N2a-Cx43 or N2a-Cx40 cell as previous described for homotypic wt Cx40 or Cx43 gap junctions.[22,26,27] An example of the exponential decay time constant (τ_{decay}) measurements at $V_j = 120$ mV from one Cx43/Cx40 cell pair is displayed in **Fig 3A**. When V_j was relatively positive on the Cx43-side of the gap junction (negative V_j pulses applied to the Cx40-expressing cell), the τ_{decay} was 7 ms and the steady-state open probability (P_{open}) was 0.14. When V_j was relative positive on the Cx40-side of the junction (negative V_j pulses applied to the Cx43-expressing cell), $\tau_{decay} = 242$ ms and $P_{open} = 0.46$. As previous described, the closing rates (inactivation gate on-rate = K_{on}) were determined by the equation:

$$K_{on} = \left(1 - P_{open}\right)/\tau_{decay}$$

and the V_j-dependent inactivation process was described by the exponential function (in ms^{-1}):

$$K_{on} = (0.0000662 \pm 0.0000116) \bullet \exp[\left(V_j - 60\right)/(15.3344 \pm 0.5122)] + (0.000253 \pm 0.0000922)$$

for the Cx40-positive and

$$K_{on} = (0.007973 \pm 0.001193) \bullet \exp[\left(V_j - 30\right)/(26.9539 \pm 0.9813)] + (-0.01708 \pm 0.004469)$$

for the Cx43-positive V_j directions.

The K_{on} values were smaller (i.e. inactivation rates were slower) when V_j was relative positive on the Cx40-side of the gap junction than when the V_j gradient was reversed. The voltage-dependent first-order on-rates for the Cx43 or Cx40 V_j positive polarities are illustrated in **Figs. 3B**, **C** and **D**.

Single gap junction channel conductance

To characterize the unitary conductance properties of heterotypic Cx43/Cx40 gap junction channels, the slope conductance between $V_j = -50$ mV and +50 mV was measured. Two different representative curves of the unitary channel activity are illustrated in **Figs. 4A and B**. In **Fig. 4A**, the unitary channel conductance (γ_j) measured 95 pS when V_j was relative positive on the Cx43 side and 122 pS when V_j was relative positive on the Cx40 side of the junction. **Fig. 4B** is another example of a recording from a different Cx43/Cx40 heterotypic cell pair which exhibited mostly 50 or 70 pS channel conductance states. The cumulative dataset of unitary gating events, obtained from 8 Cx43/Cx40 cell pairs, is summarized in a frequency histogram (**Fig. 4C**). The amplitudes of the γ_j values ranged from ~40 pS to ~130 pS, with the majority of events corresponding to ~50 and ~90 pS channels. The single-channel current–voltage (i_j–V_j) relationships, shown in **Fig. 4D**, were linearly fitted for all channel events above or below 65 pS in amplitude. The heterotypic Cx40/Cx43 gap junction channel slope γ_js were 52 pS and 94 pS.

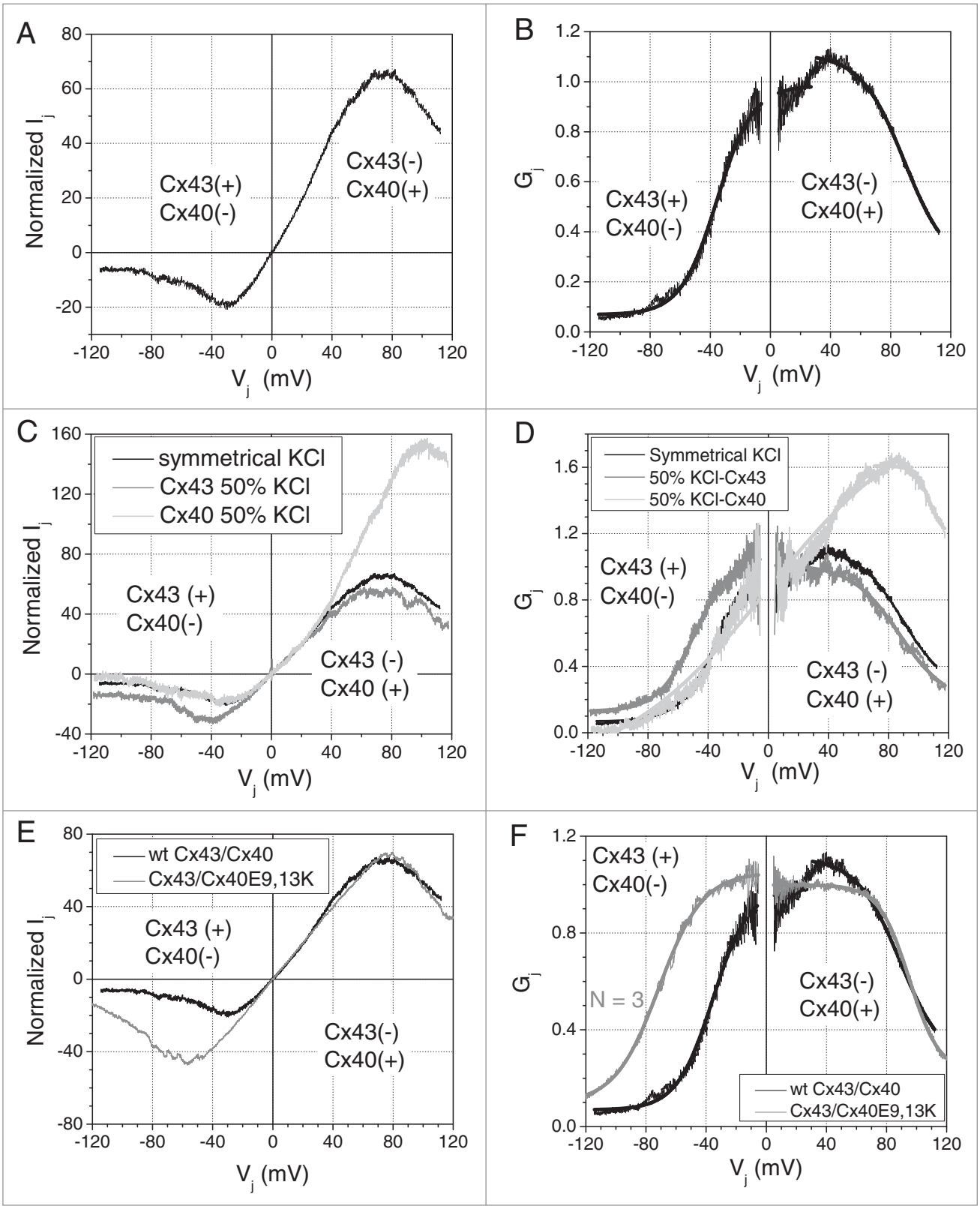

Figure 2. Normalized steady-state junctional current (**A**) and conductance (**B**) – transjunctional voltage (I_j – V_j and G_j – V_j) curves for 7 heterotypic Cx43/Cx40 cell pairs. V_j was defined relative to the N2a-Cx40 cell pair. Rectification is produced by the enhanced V_j-dependent gating on the Cx40 negative (Cx43 positive) side of the gap junction and reduced gating when the V_j polarities are reversed. Normalized steady-state I_j – V_j (C) and G_j – V_j (D) curves produced under conditions of unilateral 50% reductions in [KCl] exhibited increased rectification when low [KCl] was present on the Cx40-side and became more symmetrical when [KCl] was lowered on the Cx43-side of the gap junction (N = 6 each). Normalized steady-state I_j – V_j (E) and G_j – V_j (F) curves produced by pairing the mutant Cx40E9,13K double mutant with Cx43 dramatically reduced the rectification by reducing both polarities of V_j-dependent gating.

Table 1. V_j Gating Properties of Homotypic and Heterotypic Cx40-Cx43 Gap Junctions

Homotypic or Heterotypic Cx43 and Cx40 Gap Junctions						
Parameter	**Cx43/Cx43* $-V_j$**	**Cx43/Cx43* $+V_j$**	**Cx40/Cx40† $-V_j$**	**Cx40/Cx40† $+V_j$**	**Cx43/Cx40 $-V_j$ (<+30)**	**Cx43/Cx40$+V_j$ (>+30)**
$G_{j,max}$	1.007 ± 0.002	1.057 ± 0.002	1.040 ± 0.002	1.024 ± 0.002	0.985 ± 0.002	1.111 ± 0.002
$G_{j,min}$	0.312 ± 0.002	0.270 ± 0.002	0.163 ± 0.001	0.183 ± 0.001	0.069 ± 0.002	0.253 ± 0.009
$V_{1/2}$ (mV)	−60.1 ± 0.1	+56.5 ± 0.1	−48.8 ± 0.1	+48.7 ± 0.1	−35.5 ± 0.1	+89.2 ± 0.3
Valence (z)	1.82 ± 0.02	1.61 ± 0.01	3.31 ± 0.03	3.52 ± 0.03	2.10 ± 0.02	1.74 ± 0.03
r	0.97	0.97	0.97	0.97	0.94	0.98
N	7	7	6	6	7	7
Modified Heterotypic Cx43/Cx40 Gap Junctions						
Parameter	**50% Cx43 $-V_j$**	**50% Cx43 $+V_j$**	**50% Cx40 $-V_j$ (<+70)**	**50% Cx40 $+V_j$ (>+70)**	**43/40E9,13K $-V_j$**	**43/40E9,13K $+V_j$**
$G_{j,max}$	1.072 ± 0.005	1.013 ± 0.003	1.608 ± 0.003	1.975 ± 0.047	1.014 ± 0.001	1.004 ± 0.001
$G_{j,min}$	0.128 ± 0.003	0.175 ± 0.014	−0.254 ± 0.022	1.185 ± 0.014	0.144 ± 0.003	0.341 ± 0.004
$V_{1/2}$ (mV)	−48.8 ± 0.2	+87.2 ± 0.6	−0.7 ± 1.7	+107.1 ± 0.4	−40.2 ± 0.2	+46.5 ± 0.1
Valence (z)	2.06 ± 0.03	1.58 ± 0.04	−0.50 ± 0.02	5.23 ± 0.30	2.04 ± 0.02	3.98 ± 0.06
r	0.93	0.95	0.90	0.98	0.97	0.98
N	6	6	6	6	3	3

All parameter values are the fitted mean ± s.d.
*Homotypic Cx43 V_j gating parameters are from Lin et al.[22]
†Homotypic Cx40 V_j gating parameters are from Lin et al.[23]

Spermine block

Spermine can selectively block homotypic Cx40 gap junctions with positive V_j, but not Cx43 gap junctions.[28] To determine whether spermine can block heterotypic Cx43/Cx40 gap junctions, 2 mM spermine was added unilaterally to one cell patch pipette and the fractional block of I_j was assessed using a Δ ±10 mV, V_j pulse sequence. Owing to the asymmetrical transjunctional I-V curves, the fractional I_j block could only be calculated by comparing the normalized I_j-V_j curves in the presence or absence of 2 mM spermine as previous defined.[24] **Figs. 5A and B** illustrate the average normalized I_j-V_j curves in the presence or absence of 2 mM spermine. V_j was defined, as before, relative to the N2a-Cx40 cell. When 2 mM spermine was added unilaterally to the Cx40 expressing cell, spermine started to block heterotypic gap junction at $V_j = +40$ mV. When $V_j = +60$ mV, 2 mM spermine inhibition of I_j was 52% ± 5%, much less than the inhibition of the homotypic Cx40 gap junction by 2 mM spermine with maximum inhibition of 80% at $V_j = 50$ mV (**Figs. 5A and D**)[24]. When 2 mM spermine was added unilaterally to the N2a-Cx43 cell, spermine blocked the heterotypic Cx43/Cx40 gap junction from the Cx43 positive side of the junction (**Fig. 5C**), in contrast to the homotypic Cx43 gap junction channel. Spermine began to block the heterotypic Cx43/Cx40 gap junction at $V_j = -20$ mV (Cx43-side +20 mV) and achieved a similar maximum inhibition of 53% ± 6% when $V_j = -50$ mV (**Figs. 5B and D**). We hypothesize that spermine permeates through the Cx43 hemichannel and inhibits the heterotypic Cx43/Cx40 g_j by interacting with the Cx40 hemichannel when the Cx43-side is relative positive.

Discussion

The principal purpose of this investigation was to examine the possible formation of heterotypic Cx43/Cx40 gap junction channel in N2a cells and their biophysical properties. Our data support the conclusions that Cx40-N2a cells can form functional heterotypic gap junctions with Cx43-N2a cells and that their interactions are not mediated by endogenous Cx45, i.e., the functional contribution of Cx45 to heterotypic Cx43/Cx40 coupling in N2a cells is negligible. This conclusion is based on several observations. Firstly, the endogenous N2a cell connexin expression levels are very low. Cx40, Cx43, and Cx45 protein levels were detectable only with femtomolar sensitivity using immunoblotting methods, whereas exogenously expressed Cx43 or Cx40 proteins were at least in the picomolar range. The more sensitive RT-PCR assays further demonstrate that the relative gene expression of exogenous Cx43 or Cx40 were on par with endogenous

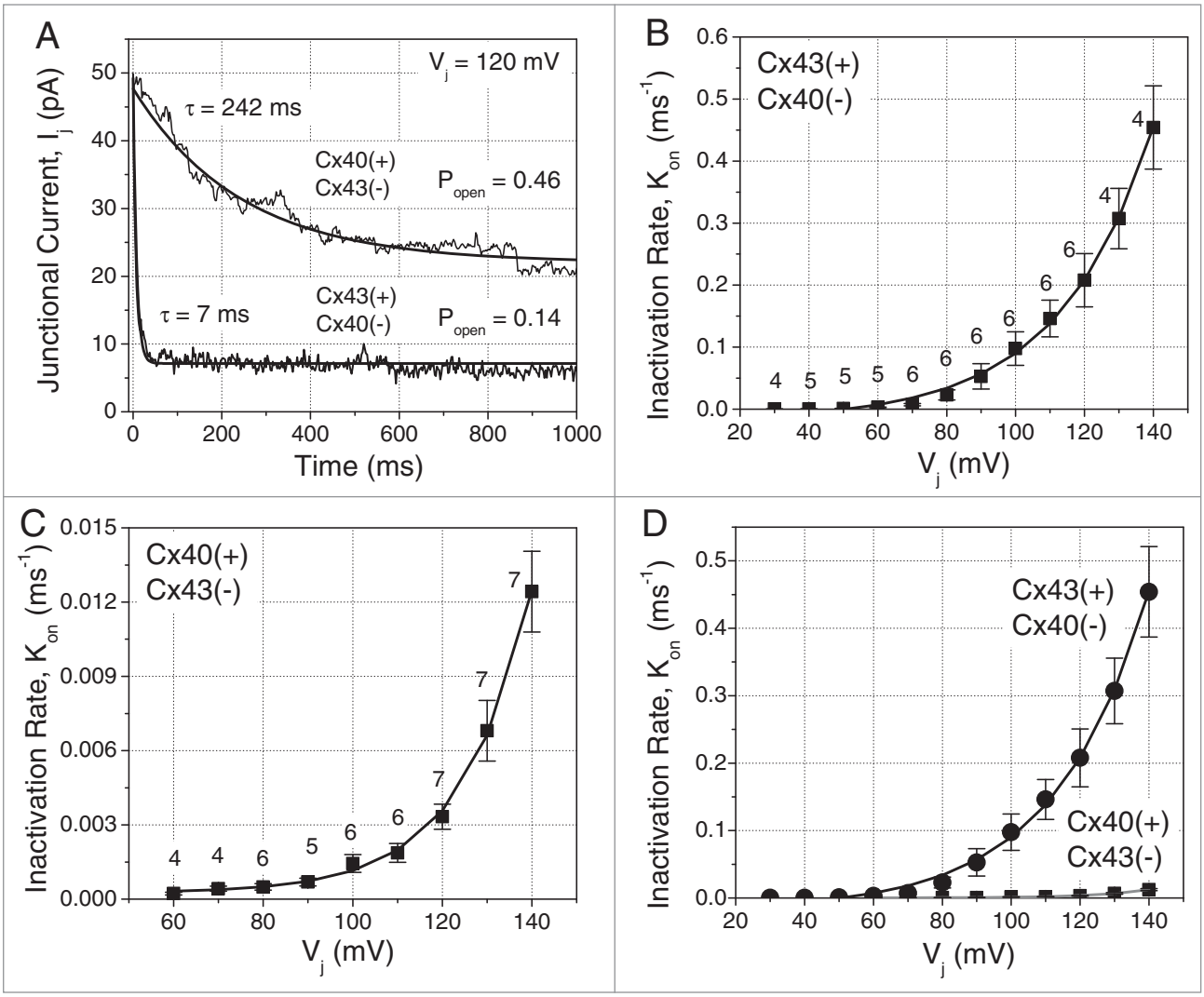

Figure 3. Kinetics of inactivation for heterotypic Cx43/Cx40 gap junctions. (**A**) Junctional current (I_j) decay time constants (τ) for a Cx43/Cx40 heterotypic cell pair when $V_j = +120$ mV relative to the Cx43 or Cx40 expressing cell. The inactivation rates were dramatically faster and the steady-state open probabilities were significantly (P_{open}) lower when V_j was positive on the Cx43-side of the gap junction. (**B**) The V_j-dependent inactivation (K_{on}) rates as determined by the equation $K_{on} = (1\text{-}P_{open})/\tau$ when V_j was positive on the Cx43-side of the junction. (**C**) The same K_{on} calculation when V_j was positive on the Cx40 side of the heterotypic gap junction. (**D**) The first-order inactivation rates for the Cx43 and Cx40 V_j positive heterotypic gap junction are plotted relative to each other. The numbers of experiments (n) are indicated next to the symbol.

GAPDH in their respective stable N2a cell clones whereas the endogenous Cx40, Cx43, or Cx45 mRNA expression levels were 1,000 to 2,000 fold lower.

Secondly, electrophysiological recordings indicate that when parental N2a cells are paired with stable Cx40-N2a or Cx43-N2a clones, electrical coupling is completely absent (data not shown). These negative results suggest that the low levels of endogenous N2a cell connexin expression are not sufficient to induce electrical coupling. Furthermore, 51% of the heterotypic Cx43/Cx40 cell pairs were not coupled (121 of 237 cell pairs tested, 39 experiments). In the remaining pairings of stable Cx43-N2a cells with stable Cx40 or mutant Cx40 E9,13K N2a cells, an average of 0.5 to 1 nS of electrical coupling developed, forming distinctly asymmetric G_j-V_j relationships. This average g_j value is approximately 4-fold lower than previously reported for the homotypic pairing of these same stable Cx43-N2a or Cx40-N2a cell clones.[22,24,26,28] Homotypic Cx40 and Cx43 pairs from these same cultures were coupled 75% and 100% of the time (n = 8). Thus, the overall coupling efficiency between stable Cx43 and Cx40 N2a cells is rather low. Thirdly, a simple series arrangement of Cx43 and Cx40 hemichannels would predict a full open state γ_j value for a heterotypic Cx43/Cx40 channel of ~120 pS(= (200*300)/(200+300) pS), given a γ_j of 100 pS for homotypic Cx43 and 150 pS for homotypic Cx40 gap junction channels. Unitary channel conductances from Cx43-N2a/Cx40-N2a cell pairs ranged from ~40 pS to ~130 pS, consistent with the existence of heterotypic Cx43/Cx40 gap junction channels.

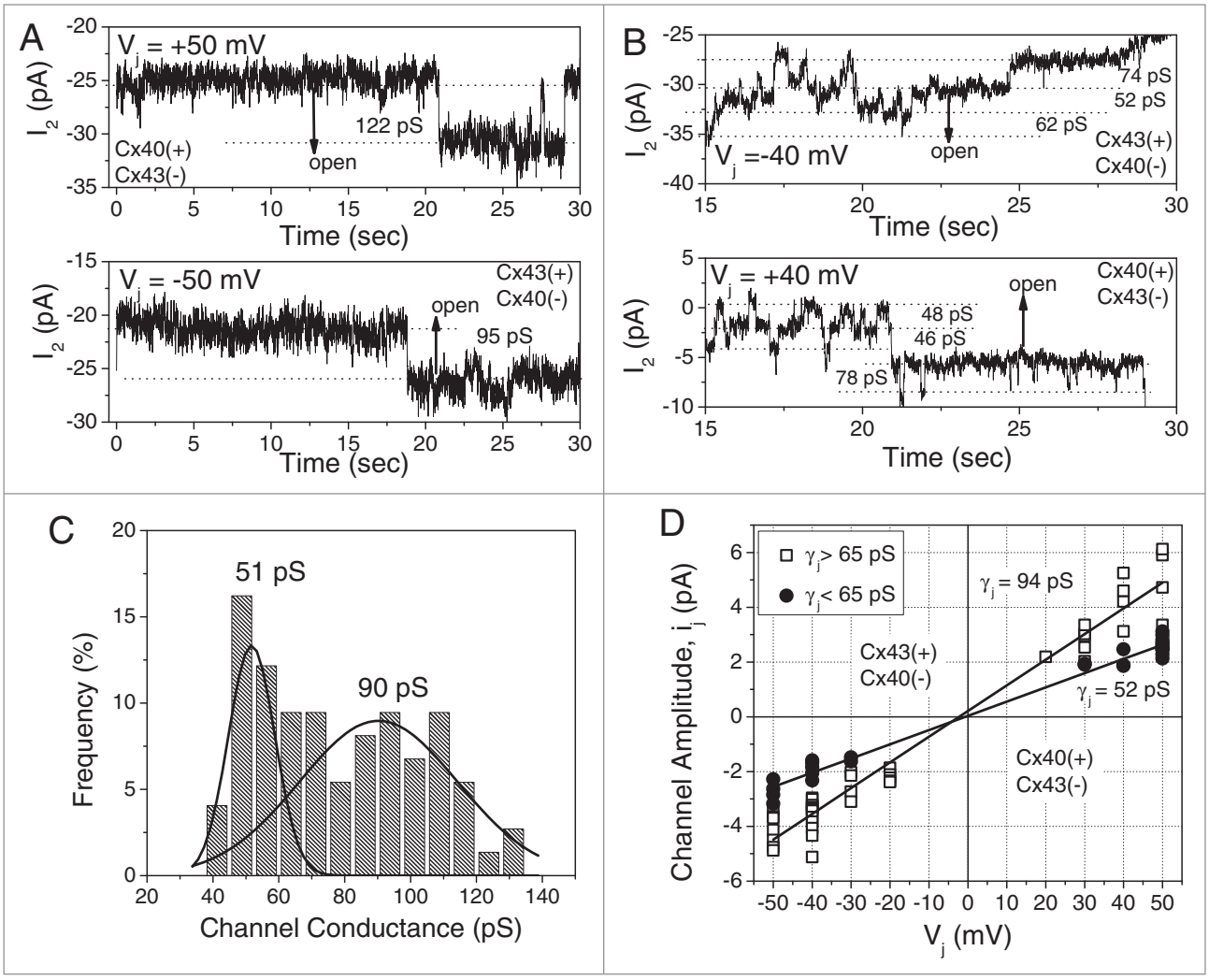

Figure 4. (**A**) Single gap junction channel currents (i_j) recorded from one heterotypic Cx43/Cx40 cell pair depicting a 120 pS channel at $V_j = +50$ mV and 95 pS channel at −50 mV relative to the Cx40 cell. (**B**) A different Cx43/Cx40 heterotypic cell pair exhibited mostly 50 or 70 pS channel conductance (γ_j) states at ±40 mV relative to the Cx40-expressing cell. (**C**) Summarized γ_j data from 8 cell pairs in a frequency histogram and multi-gaussian curve fits suggested 2 peaks at approximately 51 pS and 90 pS (N = 237 events). (**D**) The average $i_j - V_j$ relationship for 4 Cx43/Cx40 cell pairs and linear curve fits for all channel events above or below 65 pS in amplitude. These pooled channel events averaged 52 or 94 pS, indicative of Cx43 γ_j values.

Previous studies have demonstrated that heterotypic Cx43/Cx40 gap junction channels in Rin or HeLa cells possess asymmetrical steady-state g_j-V_j relationships that differ from homotypic Cx40 or Cx43 gap junctions.[11,19,20] The observed rectification occurred with negative V_j in the Cx43-containing cells. This result was attributed to the opposite gating polarities of Cx40 and Cx43, with Cx40 gating with positive polarity and Cx43 with negative polarity.[11] Opposite V_j polarities do not necessarily account for an asymmetric G_j-V_j curve since both Cx45 and Cx43 were originally proposed to gate with negative polarity, yet they form a highly asymmetric heterotypic G_j-V_j relationship.[29]

There are 2 sources for rectification of a steady state I_j-V_j curve, channel rectification, which should be evident in the instantaneous I_j or G_j-V_j relationship, and rectification due to asymmetric V_j gating. Both previous heterotypic Cx43/Cx40 gap junction reports indicated either rectification of the instantaneous G_j-V_j relationship (40%) or in the observed conductance of single channel events (20%).[11,19] Our G_j-V_j curves were produced from slow, continuous V_j ramps that result in only a steady-state G_j-V_j relationship, so no comparison is possible here. One difference between the previous and present reports is that Valiunas et al. observed "marginal or no inactivation" on the high conductance side of the heterotypic Cx43/Cx40 gap junction.[11] Using negative V_j pulses applied to the Cx40 or Cx43 cell, we routinely observed inactivation in both directions, although larger V_j gradients were required to observe the time-dependent inactivation on the higher conductance side of the junction. The variable γ_j values from experiment to experiment precluded a reliable assessment of any heterotypic gap junction channel rectification,

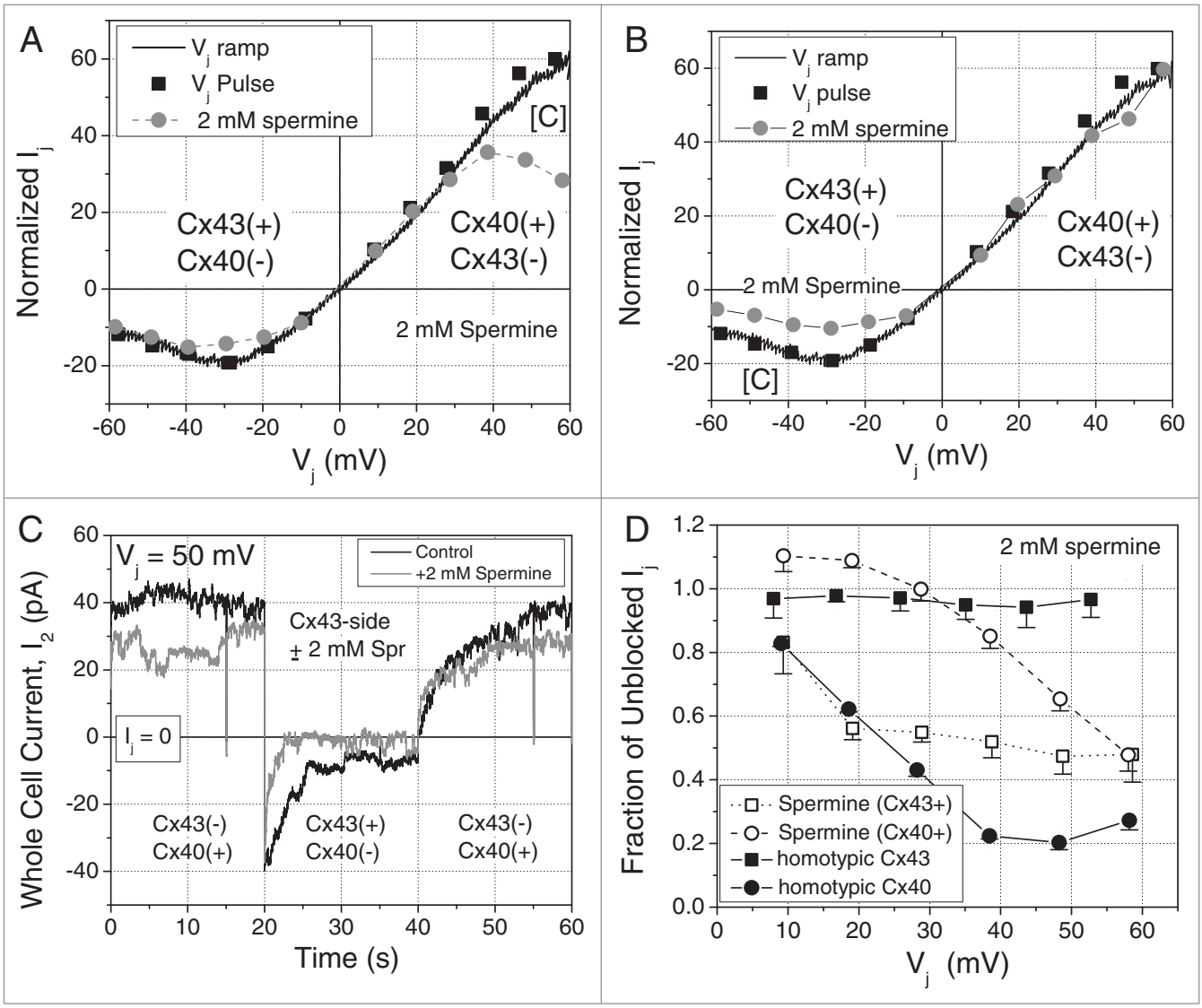

Figure 5. (**A**) Average I_j – V_j curves for heterotypic Cx43/Cx40 gap junctions obtained with symmetrical internal patch pipette solutions (black symbols and lines) or in the presence of 2 mM spermine (gray symbols and lines) added to the Cx40-side of the heterotypic gap junction. The lines indicate the steady-state curve obtained with a continuous 200 ms/mV V_j ramp and the symbols indicate the steady-state I_j value obtained at the end of a 20 sec V_j pulse to the indicated V_j value. (**B**) The same as in panel A except the 2 mM spermine was added to the Cx43-side of the heteroypic Cx43/Cx40 gap junction. (**C**) Actual current traces from 2 different experiments illustrating the effect of 2 mM spermine added to the Cx43-side of a Cx43/Cx40 heterotypic gap junction during the −/+/−50 mV V_j pulse sequence of the cationic block V_j clamp protocol. (**D**) The V_j-dependent spermine inhibition curves for homotypic Cx40 (●) or Cx43 (■) gap junctions and the heterotypic Cx43/Cx40 gap junction with spermine added to either the Cx40-positive or Cx43-positive side of the gap junction. The fraction of I_j block for the heterotypic gap junction was calculated relative to the heterotypic gap junction currents in the absence of spermine for each side of the junction.

although the only true single channel recording we obtained did reveal approximately a 20% difference in the main open channel state γ_j of 120 pS (Cx40-side positive) and 95 pS (Cx43-side positive) (**Fig. 4A**).

The asymmetry in the resultant heterotypic Cx43/Cx40 G_j-V_j relationship occurs for 2 apparent reasons. One is the voltage shift in the maximum G_j, from centered around 0 mV for homotypic gap junctions, to the 30 mV shift observed in the heterotypic Cx43/Cx40 G_j-V_j relationship (**Fig. 2B**), which was also observed for the 2 mM spermine block from the Cx40-side of the junction (**Fig. 5D**). The second factor is the asymmetry in the V_j-sensitivities for inactivation. Many studies report the $V_{1/2}$ value as an indicator of the relative sensitivity of gap junctions that vary in their connexin composition. The $V_{1/2}$ value actually refers to the V_j gradient required to produce the dynamic equilibrium between the G_{max} (main open) and G_{min} states (presumably

the residual subconductance state) and, therefore, is proportional to the energy required to effect the transition between the open and closed states in a 2-state Boltzmann distribution model. The slope of the Boltzmann curve, which is proportional to the effective gating charge valence (z), is a truer indicator of the reliance of the gating on the applied V_j gradient.

In our previous studies, we reported that the first-order inactivation voltage constants were 20 (fast) and 21 (slow) mV for homotypic Cx43 and 17.6 mV for homotypic Cx40 gap junctions.[26,27] The voltage constants in the heterotypic Cx43/Cx40 case are 26.9 mV when V_j is relative positive on the Cx43-side and 15.3 mV when V_j was relative positive on the Cx40-side. This indicates that a shift in the V_j-sensitivity of inactivation has occurred upon heterotypic pairing of Cx43 with Cx40; an increased sensitivity developing on the Cx40-positive side and reciprocal decrease in sensitivity on the Cx43-positive side of the gap junction (**Fig. 3**).

This may seem paradoxical since the rectification occurs in Cx43-positive direction, suggestive of increased V_j-gating, but this mostly results from the 30 mV Cx40-positive shift in the $G_{j,max}$. This implies that P_{open} of the heterotypic Cx43/Cx40 gap junction channel is reduced at $V_j = 0$ mV.

Decreasing the [KCl] by 50% on the Cx40-side of the junction exacerbated this asymmetric V_j shift in the G_{max} whereas a 50% [KCl] reduction on the Cx43-side of the junction moderated the asymmetry only slightly. Putative pore charge differences occur at positions 9 and 13 on the cytoplasmic NT and the first extracellular loop (E1) domains between rat Cx40 and Cx43. Negatively charged amino acid residues, E9, E13, D51, and D55, are favored in Cx40 (human Cx40 possesses an N9 residue) whereas Cx43 contains positive (K9, K13) or neutral (A51, N55) residues at these same positions. Decreasing the [KCl] by half on the Cx40 side would increase the electrostatic negative charge in this hemichannel and could be responsible for the observed V_j shift in the $G_{j,max}$. A similar effect on the Cx43 side of the junction is not observed owing to the electroneutral E1 charge substitutions and the net charge neutrality of the Cx43 NT domain. This hypothesis is supported by the heterotypic pairing of the Cx40E9,13K double mutant with wild-type Cx43 which reversed most of the apparent asymmetry in the G_j-V_j relationship (**Figs. 4E-F**). These results demonstrate that the NT charges are major contributors to the Cx40 cytoplasmic gap junction channel pore as previously reported.[25]

The formation of heterotypic gap junction channels can be affected by many different factors, such as hemichannel docking compatibility, cell-specific connexin expression patterns, the presence of cell adhesion molecules, gap junction formation rates, etc.[7,13] The functional consequences sometimes show significant variations from that of their component connexins. In this study, we demonstrate that Cx40 and Cx43 can form functional heterotypic channel in N2a cells, with different V_j-gating, unitary channel conductance, inactivation kinetic, and spermine inhibitory properties. Heterotypic Cx40/Cx43 channels also exhibit intermediate selective permeabilities relative to the 2 corresponding homotypic forms.[21] These alterations in biophysical properties of heterotypic Cx40/Cx43 channel may influence the physiology and/or pathology of the cardiovascular tissues and play a critical role in action potential propagation.

Materials and Methods

Cell cultures

Stable transfectants of mouse Neuro2a (N2a) neuroblastoma cells with rat Cx40 or with rat Cx43 were grown as previously described.[22-27] N2a-Cx40 and N2a-Cx43 cell clones were labeled with red and green lipophilic dyes (PKH26 and PKH67 kits, Sigma), respectively, according to manufacturer's instructions (**Fig. 1A**, **B**). The true color micrographs were taken with an Olympus E-420 digital SLR camera mounted to the body of an IX-70 microscope with FITC/TRITC epifluorescent illumination using a Lamda10–2 filter wheel and LS 175 W Xenon arc lamp (Sutter Instrument). In some experiments, N2a cells (80% confluent) were transiently transfected with 1 μg of Cx40E9,13K DNA for 4 hr using the pTracer-CMV2 plasmid and Lipofectamine2000 (Invitrogen), split into 2 35 mm culture dishes, and incubated overnight.[25] The green fluorescent protein-positive Cx40 E9,13K cells were co-cultured with red-labeled N2a-Cx43 cells. Heterotypic red/green N2a cell pairs were identified under epifluorescent illumination on the stage of an Olympus IMT-2 inverted phase-contrast microscope for subsequent patch clamp analysis.

Patch clamp recording

Gap junction currents were recorded in the dual whole cell configuration using conventional bath and internal pipette solutions and voltage clamp pulses or ramps as previously described.[24,30] Quantitative g_j correction methods were used to correct for series resistance errors during all patch clamp procedures according to the equation:

$$g_j = \frac{-\Delta I_2}{V_1 - (I_1 \bullet R_{el1}) - V_2 + (I_2 \bullet R_{el2})}$$

where V_1 and V_2 are the command voltage potentials, I_1 and I_2 are the whole cell currents, and R_{el1} and R_{el2} are the whole cell patch electrode resistances for cell 1 and cell 2, respectively.[30]

ΔI_2 is the change in I_2 in response to a change in V_1 (ΔV_1) and has opposite sign to the applied $\Delta V_1 \cong V_j$ gradient.

Real-time PCR

Cellular RNA was extracted with TRIzol®, quantified by UV absorption, and 500 ng total RNA was reverse-transcribed with Superscript®III™. One tenth of the cDNA reaction mix was combined with equal (nM) amounts of custom forward (5′-3′) and reverse (3′-5′) murine primers for Cx40, Cx43, Cx45, and GAPDH, Superscript® enzyme mix, and SYBR® GreenER™ dye in a 200 μl PCR tube (reaction volume = 25 μl) (Invitrogen). The samples were run for 40 cycles in a 96 well plate Bio-Rad iCycler®. All results are expressed relative to GAPDH and a cellular RNA sample without reverse transcription was run as a negative control to test for genomic DNA.[31,32]

Immunoblot analysis

Cell homogenates were harvested by scraping in ice cold phosphate-buffered saline containing a Roche mini-EDTA-free protease inhibitor tablet (per 5 ml) and 1 mM phenylmethylsulfonyl fluoride. The samples were centrifuged at 10,000 rpm for 2 min and the pellets resuspended and lysed by sonication in 25–100 μl 50 mM Tris-HCl (pH 8.0) containing 150 mM NaCl, 1% Triton X-100, 0.02% sodium azide, 50 mM sodium fluoride, 0.5 mM sodium orthovanadate, and one Roche mini EDTA-free protease inhibitor tablet. Aliquots of 1–5 μg protein, [protein] determined by the Bradford method (Bio-Rad), separated by SDS-PAGE on 10% polyacrylamide gels, blotted onto Immobilon-P membranes (Millipore), and blocked in 5% nonfat milk Tris-buffered saline (TBS), pH 7.4, overnight at 4°C. Membranes were incubated for 3 h at room temperature with rabbit polyclonal antibodies directed against amino acids 363–382 of Cx43 (Sigma, #C6219) (1:10,000 dilution) or against the C-terminal domain of Cx40 (Invitrogen, #36–4900) (1:1000 dilution).[32] Blots were rinsed repeatedly in TBS and incubated for 1 h at room temperature with a peroxidase-conjugated goat anti-rabbit IgG secondary antibody (Jackson) (Cx43, 1:5,000 dilution; Cx40, 1:5000 dilution, all in 5% nonfat milk TBS, pH 7.4). Immunoblots were developed with ECL Plus chemifluorescent reagents (GE Healthcare) and quantified using a STORM Phosphoimager.

Disclosure of Potential Conflicts of Interest

No potential conflicts of interest were disclosed.

Acknowledgments

We acknowledge Laura Andrews for technical assistance with the N2a cell cultures. We thank Dr. Steve Taffet, Department of Microbiology, for use of the Bio-Rad real-time PCR thermocycler.

Funding

This work was supported by NIH grant HL-042220 to RDV.

References

1. Schulte JS, Scheffler A, Rojas-Gomez D, Mohr FW, Dhein S. Neonatal rat cardiomyocytes show characteristics of nonhomotypic gap junction channels. Cell Commun Adhes 2008; 15:13-25; PMID:18649175; http://dx.doi.org/10.1080/15419060802014404
2. Berthoud VM, Montegna EA, Atal N, Aithal NH, Brink PR, Beyer EC. Heteromeric connexons formed by the lens connexins, connexin43 and connexin56. Eur J Cell Biol 2001; 80:11-9; PMID:11211930; http://dx.doi.org/10.1078/0171-9335-00132
3. Isakson BE, Duling BR. Heterocellular contact at the myoendothelial junction influences gap junction organization. Circ Res 2005; 97:44-51; PMID:15961721; http://dx.doi.org/10.1161/01.RES.0000173461.36221.2e
4. He D, Jiang J, Taffet S, Burt JM. Formation of heteromeric gap junction channels by connexin 40 and 43 in vascular smooth muscle cells. Proc Natl Acad Sci USA 1999; 96:6495-500; http://dx.doi.org/10.1073/pnas.96.11.6495
5. Jiang J, Goodenough DA. Heteromeric connexons in lens gap junction channels. Proc Natl Acad Sci USA 1996; 93:1287-91; PMID:8577756; http://dx.doi.org/10.1073/pnas.93.3.1287
6. Werner R, Levine E, Rabadan-Diehl C, Dahl G. Formation of hybrid cell-cell channels. Proc Natl Acad Sci U S A 1989; 86:5380-4; PMID:2546155; http://dx.doi.org/10.1073/pnas.86.14.5380
7. Koval M, Molina SA, Burt JM. Mix and match: investigating heteromeric and heterotypic gap junction channels in model systems and native tissues. FEBS Letters 2014; 588:1193-205; PMID:24561196; http://dx.doi.org/10.1016/j.febslet.2014.02.025
8. Elenes S, Martinez AD, Delmar M, Beyer$_{EC}$, Moreno AP. Heterotypic docking of Cx43 and Cx45 connexons blocks fast voltage gating of Cx43. Biophys J 2001; 81:1406-18; PMID:11509355; http://dx.doi.org/10.1016/S0006-3495(01)75796-7
9. Bukauskas FF, Bukauskiene A, Verselis VK, Bennett MVL. Coupling asymmetry of heterotypic connexin 45/connexin 43-EGFP gap junctions: properties of fast and slow gating mechanisms. Proc Natl Acad Sci USA 2002; 99:7113-8; PMID:12011467; http://dx.doi.org/10.1073/pnas.032062099
10. Rackauskas M, Kreuzberg MM, Pranevicius M, Willecke K, Verselis VK, Bukauskas FF. Gating properties of heterotypic gap junction channels formed of connexins 40, 43, and 45. Biophys J 2007; 92:1952-65; PMID: 17189315; http://dx.doi.org/10.1529/biophysj.106.099358
11. Valiunas V, Weingart R, Brink PR. Formation of heterotypic gap junction channels by connexins 40 and 43. Circ. Res. 2000; 86:E42-49; PMID: 10666425; http://dx.doi.org/10.1161/01.RES.86.2.e42
12. Moreno AP. Biophysical properties of homomeric and heteromultimeric channels formed by cardiac connexins. Cardiovasc Res 2004; 62:276-86; PMID:15094348; http://dx.doi.org/10.1016/j.cardiores.2004.03.003
13. Cottrell GT, Burt JM. Functional consequences of heterogeneous gap junction channel formation and its influence in health and disease. Biochim Biophys Acta 2005; 1711:126-41; PMID:15955298; http://dx.doi.org/10.1016/j.bbamem.2004.11.013
14. Gemel J, Lin X, Collins R, Veenstra RD, Beyer$_{EC}$. Cx30.2 can form heteromeric gap junction channels with other cardiac connexins. Biochem Biophys Res Commun 2008; 369:388-94; PMID:18291099; http://dx.doi.org/10.1016/j.bbrc.2008.02.040
15. Martinez AD, Hayrapetyan V, Moreno AP, Beyer$_{EC}$. Connexin43 and connexin45 form heteromeric gap junction channels in which individual components determine permeability and regulation. Circ Res 2002; 90:1100-07; PMID:12039800; http://dx.doi.org/10.1161/01.RES.0000019580.64013.31
16. Brink PR, Cronin K, Banach K, Peterson E, Westphale EM, Seul KH, Ramanan SV, Beyer EC. Evidence for heteromeric gap junction channels formed from rat connexin43 and human connexin37. Am J Physiol Cell Physiol 1997; 273:C1386-96;
17. Bruzzone R, Haefliger JA, Gimlich RL, Paul DL. Connexin40, a component of gap junctions in vascular endothelium, is restricted in its ability to interact with other connexins. Mol Biol Cell 1993; 4:7-20; PMID:8382974; http://dx.doi.org/10.1091/mbc.4.1.7
18. Elfgang C, Eckert R, Lichtenberg-Fraté H, Butterweck A, Traub O, Klein RA, Hülser DF, Willecke K. Specific permeability and selective formation of gap junction channels in connexin-transfected HeLa cells. J Cell Biol 1995; 129:805-17; PMID:7537274; http://dx.doi.org/10.1083/jcb.129.3.805
19. Cottrell GT, Burt JM. Heterotypic gap junction channel formation between heteromeric and homomeric Cx40 and Cx43 connexons. Am J Physiol Cell Physiol 2001; 281:C1559-67; PMID:11600419
20. Cottrell GT, Wu Y, Burt JM. Cx40 and Cx43 expression ratio influences heteromeric/heterotypic gap junction channel properties. Am J Physiol Cell Physiol 2002; 282:C1469-82; PMID:11997262; http://dx.doi.org/10.1152/ajpcell.00484.2001
21. Valiunas V, Beyer$_{EC}$, Brink PR. Cardiac gap junction channels show quantitative differences in selectivity. Circ Res 2002; 91:104-11; PMID:12142342; http://dx.doi.org/10.1161/01.RES.0000025638.24255.AA
22. Lin X, Crye M, Veenstra RD. Regulation of connexin43 gap junctional conductance by ventricular action potentials. Circ Res 2003; 93:e63-73; PMID:12946947; http://dx.doi.org/10.1161/01.RES.0000093379.61888.35
23. Lin X, Fenn E, Veenstra RD. An amino terminal lysine residue of rat connexin 40 that is required for spermine block. J Physiol 2006; 570:251-69; PMID:16284078
24. Lin X, Veenstra RD. Effect of transjunctional KCl gradients on the spermine inhibition of connexin40 gap junctions. Biophys J 2007; 93:483-95; PMID:17468172; http://dx.doi.org/10.1529/biophysj.106.098517
25. Musa H, Fenn E, Crye M, Gemel J, Beyer$_{EC}$, Veenstra RD. Amino terminal glutamate residues confer spermine sensitivity and affect voltage gating and channel conductance of rat connexin40 gap junctions. J Physiol 2004; 557:863-8; PMID:15107469; http://dx.doi.org/10.1113/jphysiol.2003.059386
26. Lin X, Veenstra RD. Action potential modulation of connexin40 gap junctional conductance. Am J Physiol Heart Circ Physiol 2004; 286:H1726-35; PMID:14693688; http://dx.doi.org/10.1152/ajpheart.00943.2003
27. Lin X, Zemlin C, Hennan JK, Petersen JS, Veenstra RD. Enhancement of ventricular gap junction coupling

by rotigaptide. Cardiovasc Res 2008; 79:416-26; PMID:18430749; http://dx.doi.org/10.1093/cvr/cvn100

28. Musa H, Veenstra RD. Voltage-dependent blockade of connexin40 gap junctions by spermine. Biophys J 2003; 84:205-19; PMID:12524276; http://dx.doi.org/10.1016/S0006-3495(03)74843-7
29. Steiner E, Ebihara L. Functional characterization of canine connexin45. J Membr Biol 1996; 150: 153-61; PMID:8661773; http://dx.doi.org/10.1007/s002329900040
30. Veenstra RD Voltage clamp limitations of dual whole-cell gap junction current and voltage recordings. I. Conductance measurements. Biophys J 2001; 80:2231-47; PMID:11325726; http://dx.doi.org/10.1016/S0006-3495(01)76196-6
31. Lin X, Gemel J, Glass A, Zemlin CW, Beyer$_{EC}$, Veenstra RD. Connexin40 and connexin43 determine gating properties of atrial gap junction channels. J Mol Cell Cardiol 2010; 48:238-45; PMID:19486903; http://dx.doi.org/10.1016/j.yjmcc.2009.05.014
32. Xu Q, Lin X, Andrews L, Patel D, Lampe PD, Veenstra RD. Histone deacetylase inhibition reduces cardiac connexin43 expression and gap junction communication. Front Pharmacol 2013; 4:44; PMID:23596417